MATERIALS CHEMISTRY FRONTIERS

REVIEW

View Article Online
View Journal | View Issue

Cite this: *Mater. Chem. Front.*, 2021, **5**, 5880

Defect engineering of molybdenum disulfide for energy storage

Zefang Yang, Lin Zhu, Chaonan Lv, Rui Zhang, Haiyan Wang, Jue Wang * and Qi Zhang *

Molybdenum disulfide, a typically layered transition metal chalcogenide, is considered one of the promising electrode candidates for next-generation high energy density batteries owing to its tunable physical and chemical properties, low cost, and high specific capacity. Optimizing electrode materials by defect introduction has attracted much attention for the design of high-performance energy devices. A great number of energy storage sites can be exposed by defect construction in electrode materials, which play a significant role in electrochemical reactions. However, there is no systematic review on the defect engineering of molybdenum disulfide materials for the energy storage process. Herein, we summarize and highlight recent advances and investigations on the defect engineering of molybdenum disulfide, with a special focus on applications in lithium-, sodium- and potassium-ion batteries. For a comprehensive illumination of defect effects, the structural defects are classified according to different geometrical dimensionalities, including point-like (vacancies, heteroatoms doping), line-like (edge site), and plane-like (interlayer) defects. Finally, we further discuss the existing challenges and future research prospects for the rational modification and design of high-performance MoS_2 electrode materials through defect engineering.

Received 20th March 2021,
Accepted 18th May 2021

DOI: 10.1039/d1qm00442e

rsc.li/frontiers-materials

1. Introduction

There is a growing demand for clean and renewable energy due to environmental deterioration and the reduction of fossil fuel reserves caused by the acceleration of the worldwide

Hunan Provincial Key Laboratory of Chemical Power Sources, College of Chemistry and Chemical Engineering, Central South University, Changsha 410083, P. R. China. E-mail: jwang79@crimson.ua.edu, qzhang1027@csu.edu.cn

Jue Wang

Jue Wang is a faculty member at the College of Chemistry and Chemical Engineering of Central South University. He received his PhD in Chemistry from the University of Alabama (UA) in 2015 under the supervision of Prof. Shanlin Pan. He then spent one year as a postdoctoral scholar in UA, following half a year in the battery industry at Contemporary Amperex Technology Co. Ltd (CATL), and recently, he completed two years of postdoctoral research at Hunan University under the supervision of Prof. Bingan Lu. His current research interests are focused on energy storage devices, including alkaline metal-ion batteries, aluminum batteries, dual ion batteries, and battery-capacity hybrid devices.

Qi Zhang

Qi Zhang received his BS and PhD degrees from the College of Chemistry and Chemical Engineering at Central South University in 2015 and 2020, respectively. He is currently a lecturer at the College of Chemistry and Chemical Engineering at Central South University. His current research interest is focused on the interfacial electrochemistry of high-energy metal anodes.

industrialization process.[1–3] Electrochemical energy storage technology with the traits of high safety, high efficiency, and environmental friendliness is regarded as the most promising candidate for next-generation clean energy storage devices.[4–6] Nevertheless, a series of intractable issues have been exposed in the innovative energy storage devices along with the progress of energy storage technology.[7] For instance, the regrettable lower energy density of rechargeable batteries has extremely restricted their pervasive application in the large-scale energy storage of renewable energy such as wind and solar energy.[8,9] In addition, the traditional electrode materials exhibit low theoretical specific capacity, sluggish kinetics for ion diffusion and electron transportation, and volume effects caused by the compulsive insertion/extraction of guest ions (Li^+, Na^+, K^+, *etc.*).[10–12] Therefore, much effort has been focused on battery design with high energy density, and there is a great need to expedite the development of electrode materials with high specific capacities, especially beyond theoretical capacities. In the past few years, thin-layer or few-layer two-dimensional (2D) materials have been favored by many researchers with the discovery of graphene, and are widely studied in numerous fields (such as semiconductor devices, catalysts and, energy storage systems) by virtue of their unique physical and chemical characteristics as compared with their bulk counterparts.[13–15] A brand-new branch has been developed for the material fields with the expeditious advancement of 2D materials, including graphene,[16,21] transition metal dichalcogenides (TMDCs),[17–19] phosphorene,[20] g-C_3N_4,[21] MXenes,[22] and layered double hydroxides.[23] Among them, TMDCs have been intensively investigated for their highly tunable crystal structures, low cost, and versatile properties.

Typically, molybdenum disulfide (MoS_2) in TMDCs presents as a sandwich structure with a layer of Mo atoms squashed between two layers of S atoms, and has been extensively investigated for rechargeable batteries in recent years because its wide interlayer structure and large specific surface area can provide abundant active sites for the reversible electrochemical reactions of guest ions with large radii.[18,24,25] Furthermore, based on theoretical and experimental results, the electrochemical energy storage mechanism of MoS_2 can be classified into two types: the intercalation reaction and the conversion reaction.[26] Interestingly, the MoS_2 electrode materials, with a capacity far beyond their theoretical values, have been reported and have aroused increasing attention.[27,28] The ''extra capacity'' may be due to the newly generated energy storage sites in the 2D layered materials and electrochemically reduced metal nanoparticles that store a large number of spin-polarized electrons in a conversion reaction.[29,30] Although MoS_2 appears to be one of the most promising candidates for electrode materials in rechargeable batteries, its practical application is still drastically hindered by some tiresome shortcomings: (1) the MoS_2 layer can aggregate due to the weak van der Waals forces between the basal planes, resulting in the reduced structure stability of the 2D nanostructures.[17] (2) The stagnant reaction kinetics of electrode materials is greatly limited by low ion- and electron conductivity. (3) The volume variation during the intercalation/extraction of exogenous ions gives rise to concomitant mechanical stress, which brings about the pulverization of the active material and the loss of contact with the current collector.[31–33] Defect engineering is one of the most fascinating and effective strategies for optimizing the structure of MoS_2 and tailoring its physical/chemical properties.[22,32] Based on the second law of thermodynamics, structural defects will inevitably perturb or even destroy the periodic crystal structure, which provokes the redistribution of chemical and electronic properties of nanomaterials.[34] According to theoretical calculations and experiments, the introduction of defects in MoS_2 electrode materials is conducive to the formation of more energy storage sites for guest ions, thus enhancing the reversible capacities.[32] Moreover, to maintain structural integrity, defective MoS_2 will affect the intercalation/deintercalation of guest ions between lamellas, decreasing the stress and electrostatic repulsion between adjacent layers, directly surmounting migration and diffusion barriers, and then promoting the diffusion of guest ions and charge transfer in electrochemical reactions.[32,35] For example, the vacancy defects introduced into MoS_2 break the periodic crystal structure, making the interlayer diffusion energy barrier only 0.085 eV as compared to defect-free MoS_2 which is prohibited interlayer diffusion.[32] Therefore, an in-depth understanding of the important role of defects, and then the introduction of preferred defects into MoS_2 clusters, is of great significance for the future development of long-lived, low-cost, and high-energy-density energy storage batteries. Nevertheless, to our knowledge, there has not been a systematic review of defect engineering in MoS_2-based materials for rechargeable batteries.

Herein, we introduce the effects of defects on MoS_2-based materials and briefly describe the characterization of the defects. The defects of MoS_2 employed in energy storage devices are classified into three categories as shown in Fig. 1, namely zero-dimensional (0D) point-like defects (vacancies, doping), one-dimensional (1D) line-like defects (edge), and two-dimensional (2D) plane-like defects. The up-to-date advances in defect engineering related to MoS_2 electrode materials in the rechargeable batteries are systematically summarized, including the lithium-ion battery (LIB), sodium-ion battery (SIB), and potassium-ion battery (PIB). We focus on the direct effects of different defect species on MoS_2 electrodes and mainly explain their influence on battery performance in combination with theoretical and experimental results. Finally, the remaining challenges and prospects in future research and development of defective MoS_2-based materials for rechargeable batteries are proposed, aiming to provide an outlook and perspective for reference in this promising field.

2. Defects in molybdenum disulfide

2.1 The characterization tool

It is very important to identify the defects and the corresponding influences on the body due to their inhomogeneity, diversity, and complexity, which can provide basic guidance for their design and the microstructure and the relationship

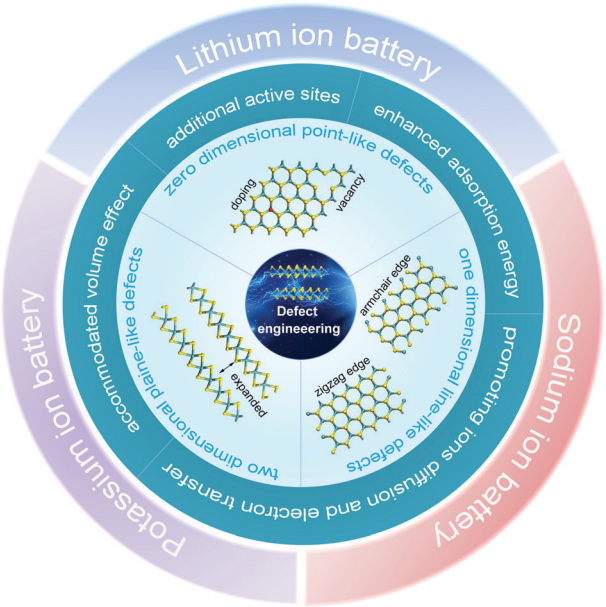

Fig. 1 Schematic illustration of the categories and effects of defects in MoS_2-based materials and their application in rechargeable batteries.

between defects and performance. Various characterization techniques have been developed to meet the needs of discovering defective electrode materials, including morphology evolution, spectroscopy techniques, and theoretical calculations. The element chemical state, the surface state, composition, crystal structure and electronic structure of MoS_2-based materials can be easily obtained through these characterization techniques. Some typical and representative characterization tools for defects are briefly introduced in the following.

Heteroatom doping is the most common way to introduce deficiencies in MoS_2, which can directly cause slim variations (lattice constants) in the bulk crystal structure and further affect the electron distribution. X-ray diffraction (XRD) can prove the evolution of pristine and treated crystal structures. As shown in Fig. 2a, the (002) plane diffraction peak of nitrogen-doped MoS_2 (N-MoS_2) is wider and more left-of-center as compared to that of bulk MoS_2, suggesting that the nitrogen doping can induce the expanded interlayer spacing and more disordered structure.[35] Raman spectroscopy can be applied to characterize the vibration state of 2D materials. Fig. 2b exhibits that the gaps in Raman spectra between the E^1_{2g} and A_{1g} peaks are 25.9 cm^{-1} for N-MoS_2, and 27.2 cm^{-1} for bulk MoS_2, which further demonstrate an expanded interlayer by the effect of nitrogen dopant.

The surface morphology, atomic arrangement and ratio, element distribution and valence, and electronic structure are also important to the electrochemical performance of MoS_2-based materials, which need to be distinctly revealed. X-ray photoelectron spectroscopy (XPS) can detect the photoelectrons generated by the excitation of the outermost electron of the atom to analyze the composition, content, and chemical state of elements. Fig. 2d depicts the N core level XPS spectra of nitrogen-doped hollow MoS_2/C nanospheres. The N–Mo bond, C–N bond, and amino group can be recognized, confirming that N is successfully doped into MoS_2 and C.[36] Also, the atomic ratio of Mo and S after the oxygen plasma treatment transformed from 1 : 1.9 to 1 : 1.38, indicating the O doping in MoS_2 nanosheets and the incorporation of vacancy defects (Fig. 2e).[37] High-resolution transmission electron microscopy (HRTEM) is a routine to characterize atomic arrangement. Typically, the bundled defect-rich MoS_2 achieved by the quenching process presents a broken periodic array of atoms and the continuously distributed vacancy defects, while pristine MoS_2 shows a consecutively ordered defect-free crystal structure (Fig. 2g).[32] The X-ray energy-dispersive spectroscopy (EDS) elemental mappings coupled with electron microscopy (Fig. 2f) can unambiguously disclose the distribution and proportion of elements, which directly indicate heteroatom doping defects.[33] Owing to the electronic structure around atoms, electron paramagnetic resonance (EPR) spectroscopy is a straightforward method to qualitatively and quantitatively identify unpaired electrons on the surface and or in the bulk of the material. Tao *et al.* investigated the 3D porous defect-rich MoS_2/C architecture for high-performance LIBs. The vacancy concentration variation determined by annealing conditions under different Ar/H_2 is shown in Fig. 2i.[38] The EPR signal and the number of S vacancy defects are significantly strengthened and broadened with the increase of the Ar/H_2 concentration.

2.2 The classification of defects with various dimensionalities

2D layered MoS_2 shows excellent electrochemical performance as compared with bulk counterparts due to its intelligently controllable morphologies and components. Specifically, further defect engineering can induce the emergence of new active sites, which generally exhibit enhanced activity for lithium/sodium/potassium ion storage. Based on geometric dimensionality, the structural defects in MoS_2 electrode materials can be classified into three categories: 0D point-, 1D line- and 2D plane-like defects.

2.2.1 Zero-dimensional point-like defects. Typically, the 0D point defects in MoS_2 mainly include vacancies and heteroatom substitution defects. The vacancies can be divided into cationic, anionic, and hybrid vacancies, which are caused by the thermal vibration of the lattice atoms in the crystal structure leaving the original sites, also known as internal defects. The existence of vacancies breaks the surroundings of atoms and distorts the crystal lattice, thus effectively regulating the electrical configuration and chemical properties of the material. Barik and Sun *et al.* calculated several vacancy formation energies based on density functional theory (DFT) through first principles, including Mo vacancies (V_{Mo}), S vacancies (V_S) and Mo and S hybrid vacancies (V_{MoS_3}) (Fig. 3a).[39,40] It was found that V_S has the lowest formation energy compared to other vacancies, which is consistent with the frequently observed experimental results. V_{MoS_3} is composed of one Mo vacancy and three upper or lower S vacancies nearby. The formation energy of V_{MoS_3} is lower than that of V_{Mo} under Mo-rich conditions, which means that once Mo vacancies are formed, the surrounding S atoms will become relaxed. The calculations revealed that the

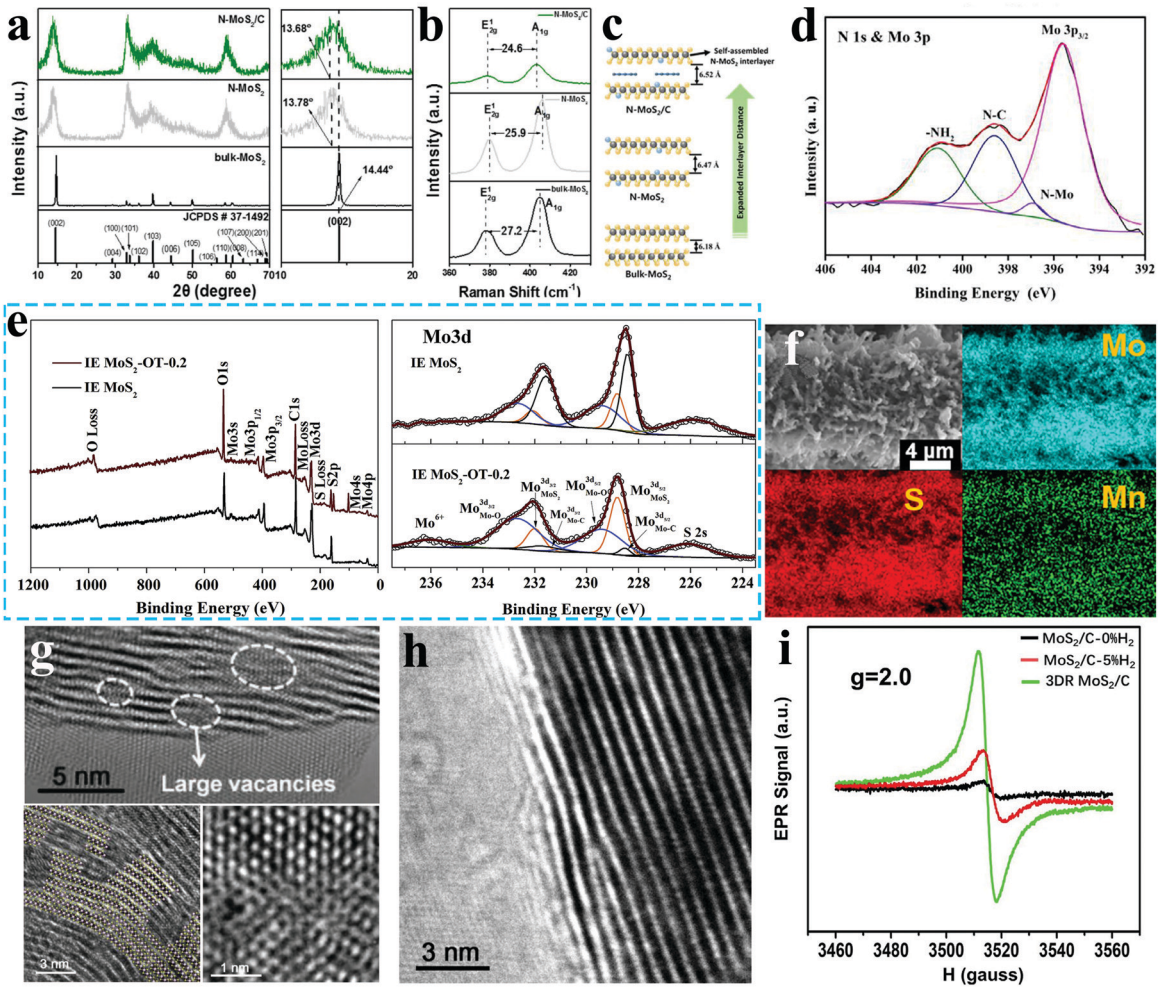

Fig. 2 The characterization of defects. (a) XRD patterns, (b) Raman spectra, and (c) structure evolution of bulk MoS_2, nitrogen-doped MoS_2 without the addition of furfural (N-MoS_2) and nitrogen-doped MoS_2/carbon (N-MoS_2/C) spheres. Reproduced with permission.[35] Copyright 2020, Elsevier. (d) XPS spectra of N 1s of the N-doped hollow MoS_2/C nanospheres prepared by the sulfuration process of Mo-MOFs. Reproduced with permission.[36] Copyright 2017, Elsevier. (e) XPS survey and Mo 3d spectra of the interlayer expanded MoS_2 with (IE MoS_2-OT-0.2) and without (IE MoS_2) treatment of oxygen plasma for 0.2 min. Reproduced with permission.[37] Copyright 2019, Elsevier BV. (f) EDS mapping for Mo, Mn, and S in Mn-doped MoS_2 nanosheets assembled by carbon nanowire arrays-decorated carbon cloth. Reproduced with permission.[33] Copyright 2019, Elsevier. HRTEM images of (g) the bundled defect-rich MoS_2 treated by quenching as-prepared MoS_2 sheet. Bottom shows different magnification and inset in the bottom-left denotes atomic model of the defect. (h) As-prepared MoS_2 sheets. Adapted with permission.[32] Copyright 2019, Wiley-VCH Verlag. (i) EPR spectra of MoS_2/C-0% H_2, MoS_2/C-5% H_2 and 3DR MoS_2/C (20% H_2) with different Ar/H_2 concentrations. Reproduced with permission.[38] Copyright 2020, Wiley-Blackwell.

existence of vacancy defects is conducive to the adsorption of alkali metal-ions (Li^+ and Na^+) in the MoS_2 materials.

Heteroatom doping by introducing substituted atoms has been proven to be a common strategy to modify the microscopic morphology, structure, and electrical properties of MoS_2 materials.[35,41,42] Heteroatoms include metallic elements and non-metallic elements. It has been reported that rational element doping can stabilize the structure, induce 2H to 1T phase transition, and improve the intrinsic conductivity of MoS_2 materials. DFT calculation was applied to investigate the effect of substituting S with nonmetal elements (N, P, As, F, Cl, and I) and Mo with metal elements (Fe, Co, Ni, Cu, and Zn) on the Li adsorption and diffusion at the MoS_2 monolayer (Fig. 3b).[43] The results show that heteroatom doping can effectively enhance the Li adsorption on the monolayer MoS_2, especially p-type doping.

2.2.2 One-dimensional line-like defects. Line-like defects are another ubiquitous type of defect engineering in 2D MoS_2 materials. Two kinds of edge-rich MoS_2 nanoribbons can be formed by cleaving MoS_2 nanosheets: armchair edge and zigzag edge.[44] Graphene with armchair edges and zigzag edges has been studied by DFT. The results show that the existence of these edges not only affects the activity of graphene nanoribbons for Li-ion adsorption but also has different diffusion properties.[45] For the MoS_2 nanoribbons, the calculation of the density of states (DOS) revealed the metallic armchair edge (Fig. 3c), which is conducive to the diffusion of Li-ions, while the zigzag edge of MoS_2 has relatively poor conductivity.[30] In addition, the MoS_2 bulk material has a strong adsorption with Li and a moderate Li diffusion barrier, and the increasing Li binding energy is often accompanied by an augmented

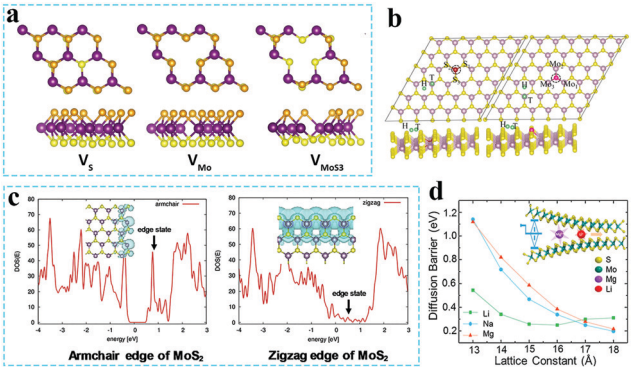

Fig. 3 The defects with different dimensionalities. (a) Optimized vacancy defects of V_{Mo}, V_S, and V_{MoS_3} in monolayer MoS_2. Adapted with permission.[39] Copyright 2019, American Chemical Society. (b) Heteroatom-doped monolayer MoS_2 with metal (left) and nonmetal atoms (right). Reproduced with permission.[43] Copyright 2018, Elsevier. (c) DOS curves and electronic structures of the armchair- and zigzag-edged MoS_2. Reproduced with permission.[30] Copyright 2018, Elsevier. (d) The relationship between the ion diffusion barrier and interlayer spacing. Reproduced with permission.[47] Copyright 2017, Elsevier.

diffusion barrier. However, the effect of increasing the ion adsorption energy while decreasing the diffusion barrier can be realized by curtailing the dimensionality from the bulk to the bilayer or monolayer. Interestingly, both the binding strength and migration of Li can be simultaneously enhanced in the rich-edge MoS_2 nanoribbons owing to the edge effect. Xia *et al.* reported that edge-rich MoS_2 nanosheets were anchored on curly N-doped graphene for high-performance lithium and sodium storage. The unique heterogeneous interfaces with high-exposed edges were connected through chemical C–O–Mo bonds, which provided high-speed ion and electron transport and enhanced electrochemical properties.[46]

2.2.3 Two-dimensional plane-like defects. For monolayer 2D nanomaterials, the adsorption of guest ions may play an important role in energy storage, and for 2D materials with few layers, the insertion and migration of foreign ions between layers is also a matter for electrochemical energy storage. In the mini-review, the expanding interlayer spacing of the lamellar MoS_2 nanosheets is defined as 2D plane-like defect engineering. A large interlayer distance can reduce the transmission energy barrier to electrons, mass, and foreign ions, especially large-radius ions, contributing to the improvement of electrochemical performance, and also buffer volume expansion, thereby heightening the structural stability during cycling (Fig. 3d).[47] Generally, small molecules, ions, particle embeddedness, heteroatom doping, and optimizing preparation methods are effective strategies for expanding the interlayered distance of the layered MoS_2.[30] Li *et al.* prepared hierarchical interlayer-expanded MoS_2 supported on carbon nanotubes *via* a straightforward solution method. The enlarged interlamellar spacing enabled better potassium-ion accommodation and a lower potassium-ion migration barrier.[48]

2.3 The effects of defects on molybdenum disulfide

Electrode materials are one of the significant constituents of batteries, whose comprehensive properties have decisive effects for the practical application of cells, such as specific capacities, cycling stabilities, and rate performances. It is known that the storage capacity of metal-ion batteries is severely limited by the number of theoretical energy storage sites of electrode materials. Rate performance is dominated by ion migration and electron transport, and the main reason for the capacity attenuation after cycling is the loss of lithium-ions caused by the continuous formation of SEI-induced volume changes. However, the crystal lattice with the incorporated defects will change pristine electronic scenarios, which is exceedingly significant for electrochemical reactions, where they can augment additional energy storage sites to provide the best activity and selectivity. It is worth noting that these defects can serve as "docking" sites to capture atomic metal species and form new synergetic coordination structures as active sites and enhance adsorption for guest ions, and also change the surrounding environment of the electrons to render fast kinetics for ion diffusion and electron transport.[49] Moreover, defect engineering can also affect the embedding and de-embedding of guest ions in the electrode materials, thus decreasing the stress and electrostatic repulsion between adjacent layers, and adapting to volume deformation. The main role of defect engineering on MoS_2 electrode materials is summarized as follows.

2.3.1 Additional active sites. Recently, it was found that the experimental capacity of MoS_2-based electrodes is usually higher than the theoretical capacity, which may be due to the additional active sites to provide more anchors for guest ions.[30] A large number of studies reported that defect engineering can greatly improve the electrochemical performance of electrode materials by affording additional active sites to generate a specific capacity higher than the theoretical value.[33,50] For instance, MoS_2–TiO_2-based composites with controllable graphene incorporation and defect engineering display improved electrochemical performances, and the defect-rich MoS_2 shell offers large amounts of additional active sites for Li-ion storage (Fig. 4a).[50] Cai *et al.* synthesized few-layer defect-rich ternary $MoS_{(1-x)}Se_{2x}$ nanosheets by using MoO_3 nanowires that were simultaneously co-etched with sulfur/selenium sources.[51] As the anode of LIBs, the as-prepared $MoS_{(1-x)}Se_{2x}$ (x = 0.25) showed a higher specific capacity than binary counterparts, which may be ascribed to appended active sites to generate extra capacity, accommodate structural change and improve conductivity. Based on this, our group designed $MoS_{(1-x)}Se_{2x}$ alloys with vacancy defects and investigated the influence of the chemical composition on vacancy concentration.[52] Both experimental and theoretical calculations demonstrated that the anion vacancy-rich $MoS_{(1-x)}Se_{2x}$ alloys could generate more active sites, mitigate structural variation and heighten electronic conductivity when being applied as PIBs anodes.

Benefiting from the special configuration of the 2D MoS_2 nanoarray, the edges of the lamella perpendicular to the (002) plane have been endowed with the advantage of enriched active sites and enhanced mass transportation. As illustrated in Fig. 4b, the horizontally disordered 2D nanoarray extends the diffusion path of Li/Na ions and has barren active sites.[53] On the contrary, there are plenty of exposed (002) edges fully

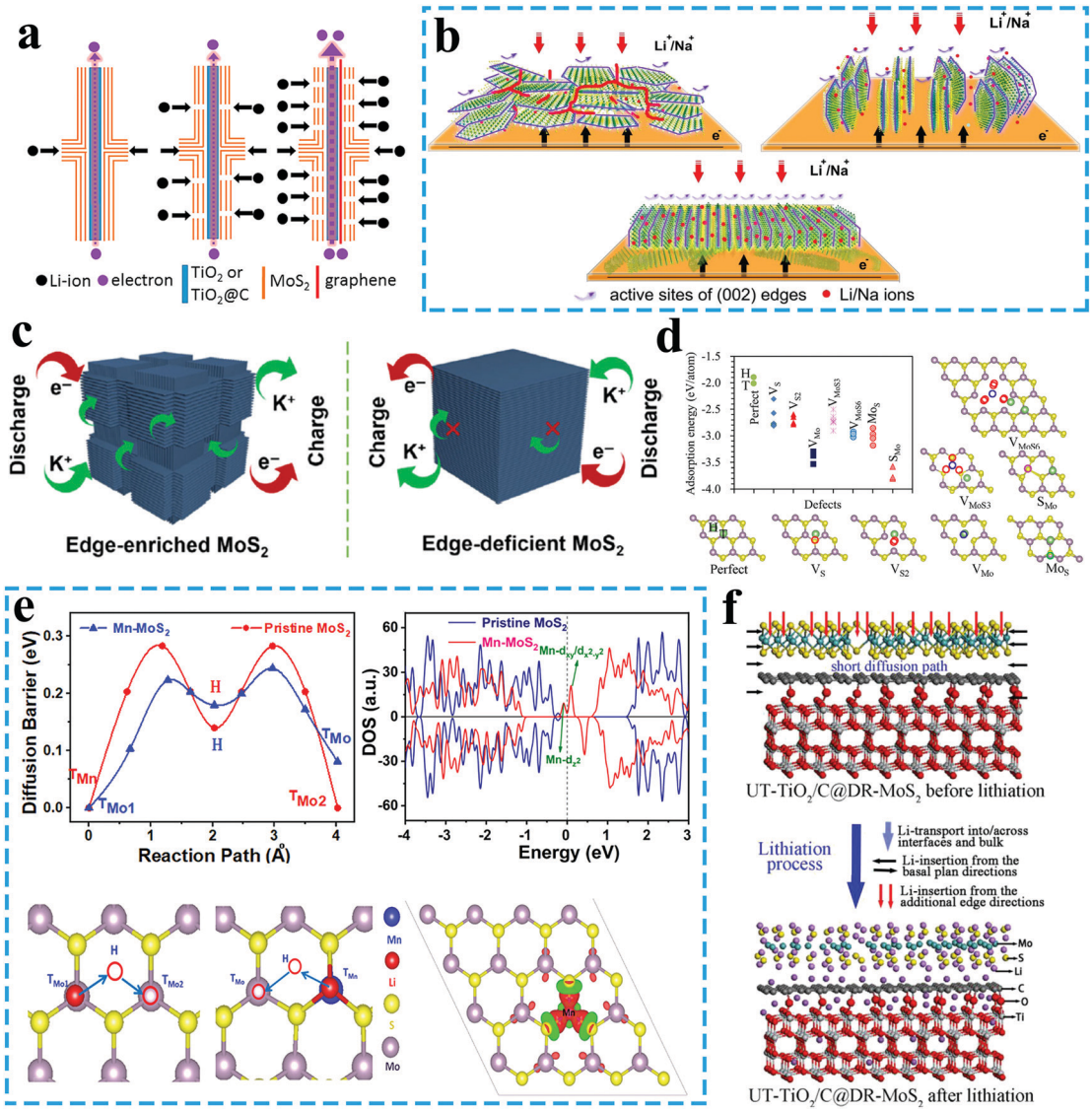

Fig. 4 The enhanced effects induced by defect engineering in MoS_2-based materials. (a) Schematic illustration of the lithium-ion and electron transport paths in MoS_2–TiO_2 anodes with different defect contents. Reproduced with permission.[50] Copyright 2017, Elsevier BV. (b) Schematic diagram of Li and Na ion transport and active site density in MoS_2 nanostructures with different sheet arrays (random order, vertically aligned arrays, and richly exposed (002) plane edges on substrates). Adapted with permission.[52] Copyright 2018, Elsevier. (c) The charge/discharge process of edge-enriched/deficient MoS_2. Reproduced with permission.[53] Copyright 2020, Tsinghua University Press. (d) The adsorption energies of Li on 2H-MoS_2 monolayer with various point defects and the most stable adsorption configurations. Reproduced with permission.[40] Copyright 2015, Nature Publishing Group. (e) The diffusion barrier of Li atoms, the DOS, corresponding atomic structure, and the charge density of MoS_2 with and without Mn doping. Reproduced with permission.[33] Copyright 2019, Elsevier. (f) The lithiation process of UT-TiO_2/C@DR-MoS_2 in the first cycle. Adapted with permission.[58] Copyright 2016, Elsevier BV.

in contact with electrolyte in the vertically aligned 2D architecture, which not only shortens the transport distance of lithium/sodium ions during the insertion/deinsertion process but also provides abundant active sites for the subsequent electrochemical reactions. Jiang and co-workers designed the edge-enriched MoS_2 (ED-MoS_2) skeleton at the mesoscale by taking advantage of the limited number of stacked layers in the framework. Numerous edge planes can be exposed on the mesopore walls, thus promoting K^+-ion diffusion kinetics and providing more accessible active sites for the electrochemical reaction.[54] In contrast, the bulky and edge-deficient MoS_2 (EE-MoS_2) exhibits undesirable active sites for K^+-ions to anchor (Fig. 4c). Therefore, the defect engineering in the MoS_2-based electrode materials can manipulate the electronic structure to provide more active sites for foreign ions to induce high capacity, by virtue of the redistribution of electrons.

2.3.2 Enhanced adsorption energy. It has been reported that sulfur vacancy defects in MoS_2 materials can improve their electrochemical activity and adsorption energy, as evidenced by the enhanced catalytic performance for hydrogen evolution reactions.[55] Therefore, the influence of the defective MoS_2 on the adsorption capabilities of alkali metal ions was further

investigated to enhance electrochemical energy storage. The DFT calculations were fulfilled by Sun *et al.* to investigate the adsorption and diffusion of lithium on monolayer MoS_2 with 0D point defects, such as single- and few-atom vacancy defects.[40] Fig. 4d shows the adsorption energy and atomistic configurations of the different defective MoS_2 with lithium atoms. The adsorption capabilities of all MoS_2 with different defects increased as compared with the pristine MoS_2, which is ascribed to the donation of Li 2s electrons to the defects to induce enhanced Li adsorption on defective MoS_2. On the other hand, based on DFT, Barik and co-workers also computed Li/Na adsorption in monolayer MoS_2 with various types of defects and demonstrated the significance of defects in enhancing the Li/Na-ion storage capability of MoS_2 monolayers.[39] Experimentally, nitrogen-doped carbon nanofiber@MoS_2 nanosheet arrays with ample S-vacancies (NC@MoS_2-VS) were exploited to serve as an anode material for SIBs through a multi-process involving electrospinning, hydrothermal, and annealing processes.[56] It was found that in the presence of S-vacancies MoS_2 can increase the adsorption energy of Na atoms and more Na atoms can be trapped on the MoS_2-VS surface combined with theoretical calculations.

2.3.3 Promoting ion diffusion and electron transportation. Both experimental and theoretical studies proved that structural defects in the MoS_2 such as heteroatom doping, expanded interlayer spacing, and various defects can regulate the dynamic process of electrons and foreign ions.[33,42,57] In recent years, it has been found that incorporating defects into MoS_2 materials can significantly improve the internal conductivity to strengthen rate performance. The insertion and diffusion behaviour of lithium in the MoS_2 with and without manganese doping deficiency were studied by Wang and co-workers using DFT calculations. As shown in Fig. 4e, there were increased electronic conductivity and accelerated ion diffusion in Mn-doped MoS_2 as revealed by metallic characteristics and a low Li^+ ion diffusion barrier.[33] Qin *et al.* reported the N-doped mesoporous molybdenum disulfide (N-MoS_2) nanosheets for enhanced lithium-ion storage performance. It was demonstrated that the resistance of lithium insertion on the electrode–electrolyte interface of N-MoS_2 nanosheets is much less than that of pristine MoS_2 nanosheets. Furthermore, there may be a conversion reaction of MoN_x to form Li_yN in the N-MoS_2 nanosheets during the lithiation process, which will enhance the ionic conductivity and facilitate lithium transfer within the electrode. The high electronic conductivity of the N-MoS_2 nanosheet can be obtained through N doping on the S-site to induce a higher density of electronic states.[57] Chen's group synthesized a Sn-doped 2H MoS_2 few-layer structure to produce a partial 1T metallic phase with abundant grain boundaries and optimized the Sn-doped concentration through a tunable formula, which endowed the 1T-2H MoS_2 hybrid with fast charge transportation.[42] Further, 2D sandwich-like carbon-coated ultrathin TiO_2@defect-rich MoS_2 hybrid nanosheets with abundant interfaces and high structural stability were reported as the anode for LIBs. Upon lithiation, the defect-rich MoS_2 with sufficient additional edge sites can shrink the diffusion path and provide more channels for Li-ions movement, facilitating the transport of Li-ions into the interfaces and deep locations of the electrode (Fig. 4f).[58] Di *et al.* demonstrated a feasible method to improve the electrochemical performances of MoS_2 electrodes through expanding its interlayer spacing. The interlamellar expansion of about 60% was induced by the incorporation of oxygen from the Mo precursor or the intercalation of NH^{4+} ions released from the decomposition of thiourea as compared to the pristine 2H MoS_2. Hence, as the anode of PIBs, the interlayer-enlarged MoS_2 not only showed better accommodation of potassium ions but also improved the diffusion kinetics of the charges during repeated potassiation and depotassiation.[48]

2.3.4 Accommodated volume effect. The uncontrollable volume variation of MoS_2 electrode materials in the electrochemical process generally leads to poor electrochemical performance, including fast capacity fading, severe voltage attenuation, and even cell failure, which has always been a tough problem for rechargeable batteries. Recently, researchers have found that the introduction of the defects in MoS_2 structures, such as heteroatom doping and expanding interlayer distance, can accommodate foreign ion integrations with less volumetric expansion and impede the re-stacking and aggregation of lamellas on the electrochemical cycling process. Li and co-workers constructed cobalt-doped few-layered 1T-MoS_2 nanosheets embedded in N,S-doped carbon nanobowls for boosting SIBs. According to experimental observation and theoretical calculations, Co-doping deficiencies play a crucial role in keeping the structural integrity. As a result, the few-layered Co-doped 1T-MoS_2 nanosheets were endowed with much lower volume expansion as compared to pristine MoS_2 and a commercial graphite anode.[68] To impede the restacking and aggregation of the 2D MoS_2 nanosheets and preserve the structural integrity during the electrochemical cycle, continuously porous microspheres were synthesized through combining defect-rich, interlayer-expanded, and few-layered MoS_2/C nanosheets. The as-prepared MoS_2/C nanosheets with robust structure can buffer the mechanical stress resulting from the volume variation upon Li-ion insertion and extraction.[59] In addition, Wang *et al.* reported interlayer-expanded MoS_2 uniformly grown on the surface of graphene by the intercalation of ammonium ions. It is worth noting that the interlayer-expanded MoS_2 weakened the van der Waals interaction between the lamella and contributed to the smooth and comfortable intercalation of Li-ions into electrode materials.[60]

Based on the above discussion, introducing structural defects with different dimensions in MoS_2 plays different roles in boosting electrochemical performance. Note that one defect usually corresponds to multiple enhancement effects, and different types of defects can also play the same role. It is desired that the comprehensive improvement of defective MoS_2 serving as electrode materials can be reached by single-defect engineering such as doping, introducing vacancies, and exposed edges. However, the 0D point defects are more conducive to creating additional adsorption sites for foreign ions and enhancing the ion adsorption, while 2D plane defects play

a crucial role in accelerating ion transmission and buffering volume changes, which suggests that the MoS_2 with exposed interlayer distance is in favor of large-radius ion transport. Therefore, the suitable defect designs in MoS_2 electrode materials should be judged in advance for different electrochemical energy storage systems.

3 Applications of defective molybdenum disulfides in energy storage

The defective MoS_2 materials with unique structure and compositional features were endowed with special characteristics, such as extra electrochemical active sites, strengthened adsorption for foreign ions, high conductivities, and enlarged interlayer spacing, which render them attractive candidates in various energy storage systems. In this section, the recent developments in MoS_2 electrode materials with different types of defects for electrochemical energy storage are summarized, including lithium-ion batteries, sodium-ion batteries, and potassium-ion batteries, and the enhanced physical and chemical properties induced by defects are emphasized.

3.1 Lithium-ion battery

In recent years, due to the unique 2D morphology and fascinating properties of nanostructured MoS_2 materials, it has become a suitable host among the numerous candidates for the anodes of LIBs. However, some intrinsic shortcomings greatly limit its practical application, such as weak van der Waals force connections between the basic planes, low conductivity, and volume changes during charge and discharge, which lead to the conspicuous degradation of the electrochemical performance. Defect engineering has been proven to be a general strategy to mutate the microscopic morphology and modulate the electronic structure of MoS_2 nanomaterials, resulting in improved electrochemical performances.

For instance, Qin *et al.* reported N-doped mesoporous MoS_2 nanosheets with enhanced Li storage performance. Upon lithiation, Li_3N formed by the high concentration of N doping can enhance ionic conductivity to reduce polarization, thus delivering excellent stability (capacity reservation of 998 mA h g^{-1} after 100 cycles).[57] Liu *et al.* prepared N-doped O-rich MoS_2 nanosheets through simple two-step methods, including the preparation of defective MoS_2 by a hydrothermal method, followed by annealing in an ammonia atmosphere. Combined with theoretical calculations, there was the reorganization of the electronic structure and shortening of the bandgap in N-doped MoS_2 to show a higher Li-storage capacity than the pristine MoS_2.[61] Besides, in order to improve the overall performance of MoS_2, a defect-enriched $MoS_{2(1-x)}Se_{2x}$ with tunable S and Se ratio was prepared to optimize the electronic conductivity of the composites conducted by Cai *et al.* The incorporation of Se not only increased the active sites for Li storage and improved the electronic conductivity, but also expanded the interlayer spacing and exposed more active edges to provide a convenient channel for Li-ion transmission. These profitable features endowed $MoS_{2(1-x)}Se_{2x}$ (x = 0.25) with outstanding electrochemical performance with the retention of the highly reversible capacity as shown in Fig. 5a and b.[33] Considering that MoS_2 treated by oxygen plasma can simultaneously generate vacancies and doping defects, a large amount of oxygen was incorporated into the expanded-interlayer MoS_2 by plasma treatment with an exposure time of 0.2 min (IE MoS_2-OT-0.2) to form a stable Mo–O–C connection (Fig. 2e). The vacancies, heteroatom defects, and Mo–O disordered domains induced by oxygen plasma treatment can cause additional active sites for Li-ions and enhance the structural stability during the cycle (Fig. 5c). Benefiting from these advantages, the IE MoS_2-OT-0.2 electrode exhibited superior electrochemical performance with long-term stability as compared to plasma-treated MoS_2 with different exposure times and untreated without MoS_2 (Fig. 5d and e).[37]

In order to solve the lamellar aggregation and restacking of layered MoS_2, the morphology, microstructure, and Li storage performance of Co-doped MoS_2/reduced graphene oxide hybrids (Co-doped-MoS_2/RGO) were investigated by Xu and co-workers.[41] It was found that rational Co doping can change the microscopic morphology (Fig. 5f and g) and structure of hybrids, resulting in improved electrochemical lithium storage performance. Compared with undoped MoS_2/RGO, Co-doped-MoS_2/RGO-2 with mole ratio of Co : Mo = 1 : 4 delivered a higher initial capacity (1385.3 mA h g^{-1} *vs.* 1382.6 mA h g^{-1}) and improved initial coulombic efficiency (ICE, 89.2% *vs.* 67.2%) as shown in Fig. 5h and i. The high reversible capacity was realized by the optimized mole ratio of Co and Mo in Co-doped-MoS_2/RGO (Fig. 5j). Li's group reported Mn-doped MoS_2 nanosheets anchored on the carbon nanowire array-modified carbon cloth (MMSC) to optimize the hierarchical structure to hinder the aggregation of MoS_2 nanosheets and enhance the transmission of electrons and ions. Mn-doping acts as an electron donor to donate electrons into MoS_2 to induce internal charge redistribution, endowing the MMSC nanosheets with metallic features to enhance charge transmission (Fig. 4e), thus resulting in enhanced rate performance. The MMSC nanosheet electrode delivered a robust long cycle life and rate performance as the anode of LIBs (750 mA h g^{-1} at 1 A g^{-1} over 1000 cycles).[56] Also, Sn and Fe-doped MoS_2 can induce the partial transformation of the 2H phase to 1T and extend the interlayer spacing, which accelerates electron transfer and ion diffusion and affords superior electrochemical performance.[62,63] In fact, the 2D diffusion of Li ions along the MoS_2(002) basic plane is easier, but the migration between the defect-free MoS_2 layers is prohibited, especially for large-radius ions. Therefore, the 3D diffusion of foreign ions along the interlayer is greatly important for fast kinetics. Tao *et al.* reported morphology engineering associated with tunable defects to synthesize defect-enriched few-layer MoS_2 nanosheets for Li storage.[38] According to DFT calculations, the energy barrier for Li-ions to pass through the double-vacancy-defect MoS_2 layer is only 0.238 eV, which is much lower than the zero-defect (3.14 eV) and single-defect (7.97 eV) MoS_2 (Fig. 5k). Furthermore, Tan and his group proposed a towel-like O-incorporated MoS_2 nanosheet vertically oriented anchored on

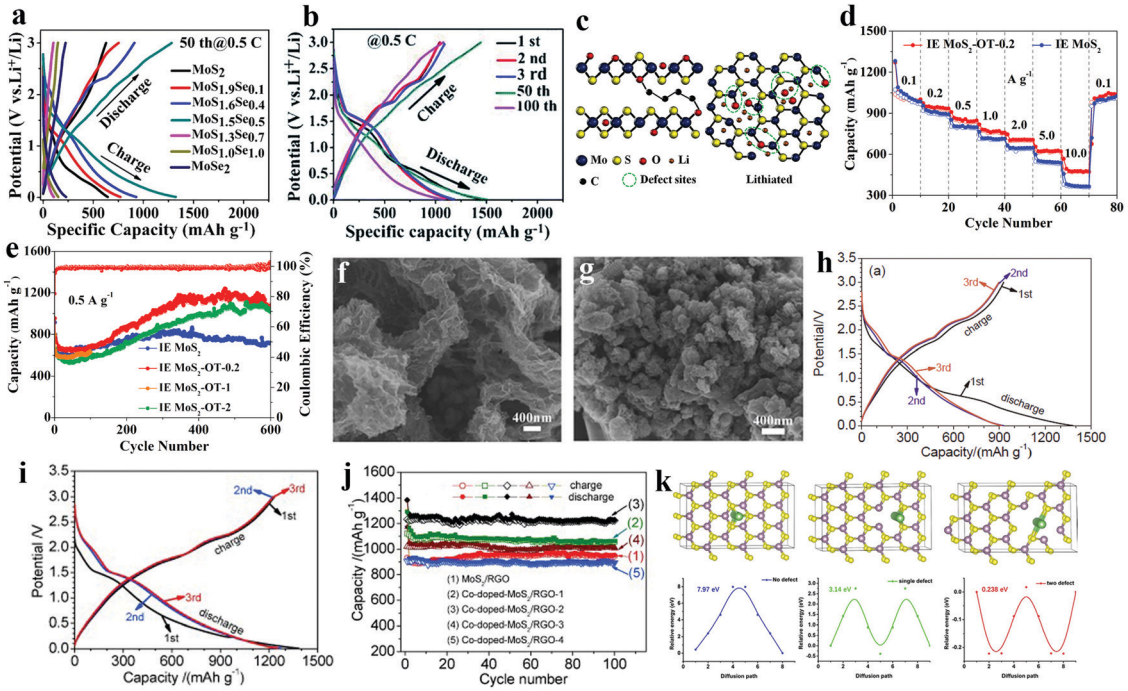

Fig. 5 The defective MoS_2 electrode for high performance LIBs. Galvanostatic charge–discharge voltage profiles of (a) $MoS_{2(1-x)}Se_{2x}$ for the 50th cycle, and (b) $MoS_{2(1-x)}Se_{2x}$ (x = 0.25) for the different cycle states at a current density of 0.5C. Reproduced with permission.[51] Copyright 2019, Royal Society of Chemistry. (c) Schematic illustration of lithiation process for the distorted structure. (d) Rate performance of IE MoS_2-OT-0.2 and IE MoS_2. (e) Cycling stability of IE MoS_2-OT-0.2, IE MoS_2-OT-1, IEMoS_2-OT-2, and IE MoS_2 electrodes at a current rate of 0.5 A g^{-1}. Reproduced with permission.[37] Copyright 2019, Elsevier BV. SEM images (f and g) and galvanostatic charge–discharge voltage profiles (h and i) for the first three cycles at a current density of 100 mA g^{-1} of (f and h) MoS_2/RGO and (g and i) Co-doped MoS_2/RGO-2. (j) Cycling performances of MoS_2/RGO with varied Co dopant. Reproduced with permission.[41] Copyright 2018, Elsevier BV. (k) The Li-ion diffusion model on the MoS_2 monolayer with different types of defects (zero defect, single defect and double defect) and corresponding energy potential curves. Reproduced with permission.[38] Copyright 2020, Wiley-Blackwell.

curly N-doped graphene (MS@N-G).[46] The ion diffusion barrier in MoS_2 nanosheets was reduced by the rich edge and expanded interlayer spacing. There was enhanced electron transmission in the heterogeneous interface between MoS_2 and graphene connected by a chemical bond (C–O–Mo) so that excellent electrochemical performance is given (a capacity of 675 mA h g^{-1} at 500 mA g^{-1} after 450 cycles). Teng *et al.* designed MoS_2 nanosheets grown vertically on graphene as the anode of LIBs to deliver a stable and long life even in harsh temperature environments (−20 °C).[64] The outstanding performance is attributed to the abundant active sites provided by the vertical growth of MoS_2 and accelerated the electron transfer induced by the C–O–Mo bond from graphene to MoS_2. Hence, the as-prepared edge-exposed MoS_2 with expanded interlayer spacing can facilitate the adsorption of foreign ions, shorten the diffusion path of ions and accelerate the insertion/extraction of ions. When vertical orientation and interlamellar distance regulation are simultaneously applied, the electrochemical performance of MoS_2 electrodes is expected to be effectively enhanced and improved.

3.2 Sodium-ion battery

Sodium-ion batteries have attracted plenty of attention in recent years as an alternative energy storage system for LIBs owing to the abundant sodium resources in nature and potentially low cost. However, there are some disadvantages to block the rapid advancement of SIBs, such as Na ions with a larger radius than Li, the stagnant Na-ion diffusion kinetics, and large volume variation during sodiation, which result in capacity decline and low coulombic efficiency.[35] Unfortunately, it was found that Na-ions were difficult to embed into the internal lattice of graphite used in the anode of the commercial LIBs and only an experimental capacity of 36 mA h g^{-1} was gained.[65] Recently, MoS_2 with the 2D layered structure has been considered as a suitable sodium ion host material due to its large interlayer spacing.[66,67] Although MoS_2 has some shortcomings, such as low internal electronic conductivity, volume expansion associated with the conversion reaction, and slow ion transport, reasonable defect engineering can completely solve the above challenges, making it a potential candidate for the anode materials of SIBs.

Lim and co-workers synthesized self-assembled N-doped MoS_2/C spheres by taking advantage of the self-doping effect of thioacetamide as a sulfur and nitrogen co-source and the self-polymerization characteristics of furfural as a carbon source in a naturally formed acidic catalytic reaction without any additives and surfactants. The doped defects and enlarged interlayer spacing introduced by N doping not only provided enough active sites for Na-ions but also accelerated the charge transport. The unique structure showed improved electrochemical performance as the anode of SIBs, such as the high

capacity of 387.9 mA h g^{-1} at 10C rate and high-rate cycling (*i.e.*, capacity retention of over 96% even after 100 cycles at 1, 2, and 5C-rate).[35] Cai *et al.* synthesized N-doped hollow MoS_2/C nanospheres and demonstrated excellent electrochemical sodium storage performance with an unexpectedly reversible capacity of 128 mA h g^{-1} after 5000 cycles at 2 A g^{-1} with a capacity fading rate of 0.036% per cycle.[36] Li and co-workers constructed few-layered Co-doped 1T MoS_2 nanosheets embedded in N,S-doped carbon nanobowls, in which Co doping plays an important role in preserving the structural integrity in the electrochemical cycling. Both for the Co-doped and original MoS_2 structure, it was found that the volume expansion of Na atoms entering the former was only 4.88%, which was much lower as compared to the latter and commercial graphite anodes, as evidenced by first-principles calculations. By virtue of the synergistic effects of the stable structure, the hybrid exhibited excellent rate performance and superior cycle stability with an achieved capacity of 235.9 mA h g^{-1} even at 25 A g^{-1} and preservation of 218.6 mA h g^{-1} even over 8240 cycles at 5 A g^{-1}.[68] As mentioned above, the guest ions can only enter the defect-free MoS_2 from the edge of the sheet and diffuse along with the layer, which is detrimental for 3D diffusion. In order to realize fast dynamics for 3D diffusion, a unique structure of bundled defect-rich MoS_2 (BD-MoS_2) was reported by Yao and co-workers (Fig. 6a). When BD-MoS_2 was employed as the anode of SIBs, Na ions diffused through the vacancies along the interlayer rather than along the lamellar plane, indicative of shorter and more diffusion paths. It was found that the interlayer spacing of the defective lattice was expanded to 0.98 nm in the processes of Na ions being embedded into MoS_2 (Fig. 6b), while the indefective lattice was 0.68 nm, suggesting that Na ions easily diffused in through vacancies the body. As a result, the bundled architecture blocked the stacking of sheets with outstanding cycle life illuminating the highly reversible capacities of 350 and 272 mA h g^{-1} at 2 and 5 A g^{-1} after 1000 cycles as shown in Fig. 6c.[32]

Although heteroatom doping and vacancy defects are the most common defect engineering, currently, some reports have

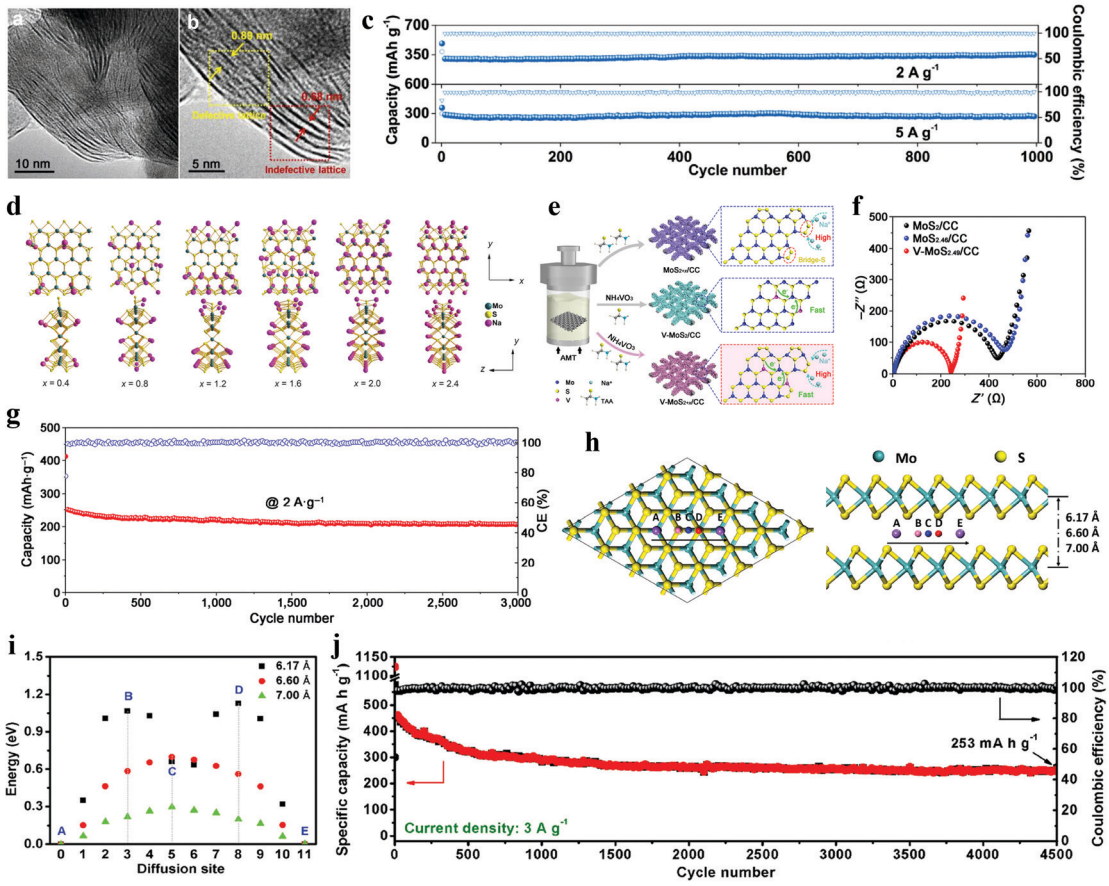

Fig. 6 The defective MoS_2 electrode for high performance NIBs. (a and b) High-resolution TEM images of the BD-MoS_2 electrode after discharge to 0.65 V. (c) Long-term cycle properties of the BD-MoS_2 at 2 and 5 A g^{-1}. Reproduced with permission.[32] Copyright 2019, Wiley-VCH Verlag. (d) Structural illustration of different amounts of Na adsorbed on both sides of S-saturated MoS_2NRs (corresponding to the normal formula of Na_xMoS_2, x = 0.4, 0.8, 1.2, 1.6, 2.0, and 2.4). Reproduced with permission.[69] Copyright 2017, Wiley-Blackwell. (e) The preparation process and Na storage mechanism and (f) EIS spectra of the MoS_{2+x}/CC, V-MoS_2/CC, and V-MoS_{2+x}/CC. (g) The cycle life of V-$MoS_{2.49}$/CC at 2 A g^{-1}. Reproduced with permission.[70] Copyright 2021, Tsinghua University Press. (h) Schematic illustration of the diffusion of Na atoms between MoS_2 layers with different interlayer spacings. (i) The corresponding diffusion barrier curve. (j) The long-term cycle performance of G@MoS_2–C nanosheets at 3 A g^{-1}. Reproduced with permission.[66] Copyright 2018, Wiley-Blackwell.

demonstrated that edge engineering and expanded interlayer building are also prevalent in layered MoS_2. The comprehensive studies conducted by Chen's group compared the adsorption and diffusion of Na on S-saturated zigzag MoS_2 nanobelts (MoS_2 NRs) and bulk MoS_2 based on DFT calculations.[69] Considering the double adsorption and edge adsorption models, the maximum theoretical capacity of MoS_2 NRs (386.4 mA h g^{-1}) was predicted to be higher than that of bulk MoS_2 (146 mA h g^{-1}) and single-side adsorption (209.3 mA h g^{-1}) for Na tends to adsorb on both sides of the nanoribbons to reduce electrostatic repulsion (Fig. 6d). The special configuration with the S atom saturated Mo edge provides extra adsorption sites to contribute additional capacity, which stabilizes the free-standing nanoribbons as well as increases the capacity. The diffusion barrier on MoS_2 NRs (0.17 eV) was calculated to be much lower than that of bulk MoS_2 (1.15 eV), suggesting prominent diffusion kinetics. On the other hand, edge engineering based on bridge-sulfur in MoS_2 can react with Na ions to achieve a reversible conversion between bridge sulfur and sodium sulfide, and heteroatom doping can effectively regulate the electronic structure to control the conduction behavior. Combining the above dual co-modification feature, Dong *et al.* experimentally reported supersaturated bridge-sulfur and vanadium co-doped MoS_2 nanosheets on carbon cloth (V-$MoS_{2.49}$/CC) *via* the hydrothermal method for enhanced sodium storage performance (Fig. 6e).[70] Benefiting from the synergistic effect of bridge sulfur and V doping, the V-$MoS_{2.49}$/CC anode was endowed with additional specific capacity and improved internal conductivity (Fig. 6f), which achieved a reversible capacity retention of 83% after 3000 cycles at 2 A g^{-1} (Fig. 6g).

Despite the vacancies in MoS_2 that can realize the 3D diffusion behaviour of Na ions, the few-layered MoS_2 with extended interlayer spacing has a more accessible surface area and lower ion diffusion resistance to achieve fast diffusion kinetics between layers through 2D diffusion in the interlayer. In addition, the acceleration of charge transmission can be done by shortening the ion diffusion length and electron transport distance to tailor the reversible reaction that occurs on the surface or near the surface of the electrode material. Zhao and co-workers reported the design and synthesis of graphene@MoS_2 sandwich nanostructures, in which MoS_2 is strongly coupled to graphene nanosheets (G@MoS_2–C). The unique 2D sheet-like G@MoS_2–C structure with extended interlayer spacing shortens the ion diffusion length and reduces the ion diffusion resistance revealed by the DFT calculation to prove a smaller energy barrier (Fig. 6h and i). The G@MoS_2–C exhibited superior long-term cycle stability (a high reversible capacity of 253 mA h g^{-1} after 4500 cycles as shown in Fig. 6j) and outstanding rate performance (the high rate capacities of 152 and 93 mA h g^{-1} at 30 and 50 A g^{-1}) as the anode of SIBs owing to the ultra-high surface or near-surface reaction contribution.[66] Dong *et al.* prepared MoS_2 with interlayer spacing expanding to 1 nm by a simple hydrothermal route at low temperature, which accelerated the transfer/transport of charge as evidenced by the alleviation of diffusion limitation.[67]

3.3 Potassium-ion battery

Potassium-ion batteries have been vigorously studied and are expected to be used in the large-scale energy storage industry due to the more abundant potassium sources as compared to lithium, the similar working mechanism of LIBs and SIBs, and the more negative redox potential than sodium (K^+/K = 2.93 V, Na^+/Na = 2.71 V *vs.* standard hydrogen electrode). However, the size of K^+ brings great challenges to ion diffusion and often results in poor dynamic performance. Much insight has been gained by researchers in recent years on the 2D lamellar MoS_2, being an easy 2D topological extension, d due to its high potassium storage capacity. Although MoS_2 cannot escape the fate of low conductivity, volume expansion, and structural degradation upon the insertion/extraction of K^+, it is encouraging that the existing MoS_2 modification strategy (defects engineering) for LIBs and SIBs may be transplanted to improve the electrochemical performance of PIBs.

In our previous work, $MoS_{2(1-x)}Se_{2x}$ with adjustable anion vacancy concentration (Fig. 7a) was synthesized through a simple alloy reaction. The optimized vacancy-rich MoSSe was energetically conducive to the adsorption of K and showed a lower volume variation than the defect-free MoS_2 during the potassium storage process as evidenced by DFT calculations (Fig. 7b and c). More active sites were induced by vacancies to contribute fast kinetic reactions. As a result, the outstanding electrochemical performances with a high reversible stable capacity of 220.5 mA h g^{-1} at 2000 mA g^{-1} after 1000 cycles were received when vacancy-rich MoSSe was used as the anode of PIBs (Fig. 7d).[51] In order to enhance the K-ion diffusion kinetics and increase the accessible reactive sites for the conversion reaction, a comparison of the K absorption and diffusion at the enriched edge (EE-MoS_2) and edge-deficient MoS_2 (ED-MoS_2) through DFT calculations was conducted by Jiang *et al.* It was found that EE-MoS_2 had the stronger K adsorption capacity and lower diffusion energy barrier as compared to ED-MoS_2, implying the rapid kinetics of ion diffusion in rich-edge MoS_2. Electrochemical measurements revealed that EE-MoS_2 possessed a lower polarization voltage, high ICE, and improved reversible capacity as compared to ED-MoS_2, which may be attributed to the effects of plenteous edge planes to reduce polarization and buffer undesirable side reactions.[53]

Recently, since the interlayer galleries are capable of accommodating foreign ions with large radii, such as K^+ ions, much effort has been devoted to expanding the interlayer spacing of MoS_2 to realize the reversible disembeddedness of K^+-ions. Di and co-workers reported the interlayer-expanded MoS_2 (exp-MoS_2) assemblies to enhance electrochemical potassium ion storage. The MoS_2 with an interlayer spacing of 0.98 nm can be synthesized by kinetically freezing the nanostructure at the initial stage of growth before the formation of a thermodynamically stable 3D crystal, as revealed by XRD analysis. In contrast to the normal interlayer distance (0.62 nm), the interlamellar expansion effects endow MoS_2 with fast and steady electrochemical storage of K ions at reversible capacities of 510 mA h g^{-1} after 100 cycles.[48] Based on DFT calculations

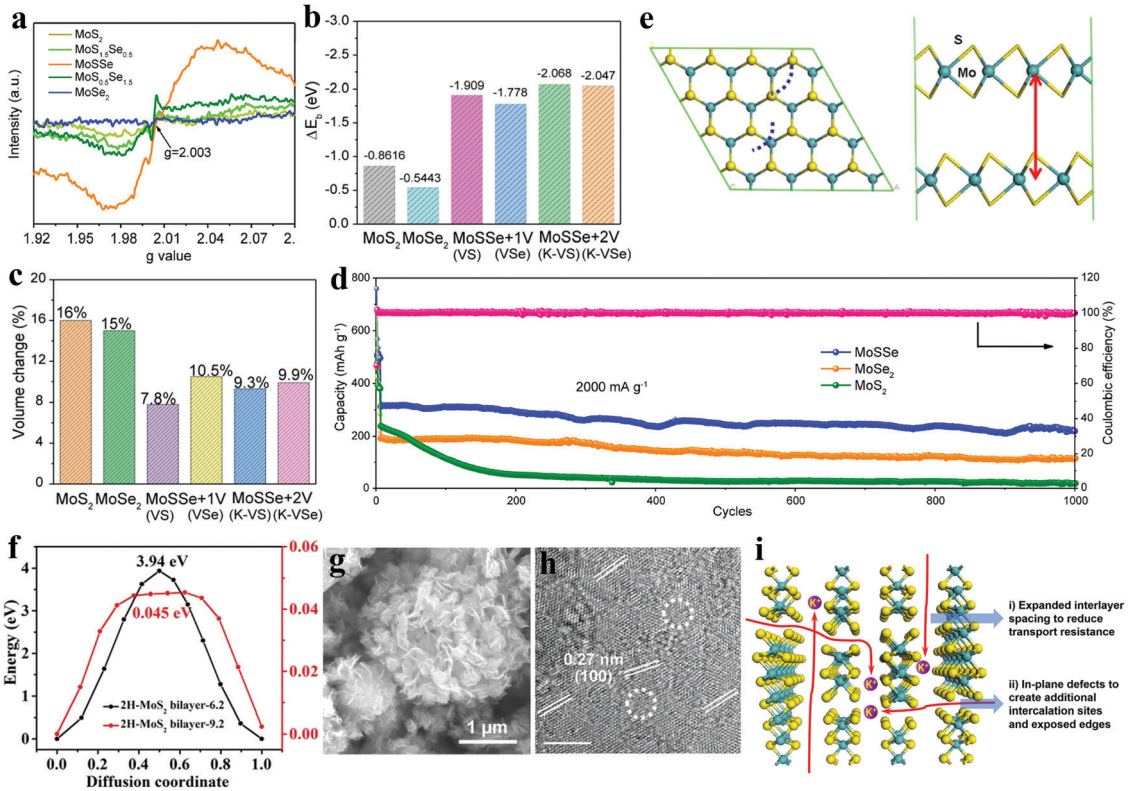

Fig. 7 The defective MoS_2 electrode for high-performance KIBs. (a) EPR analysis of as-prepared $MoS_{2(1-x)}Se_{2x}$, (b) Binding energy (ΔE_b) and (c) volume change during potassium storage for all calculated models. (d) Cycling performance for $MoSe_2$, MoSSe, and MoS_2 at 2000 mA g^{-1}. Reproduced with permission.[51] Copyright 2019, American Chemical Society. (e) The diffusion structures of Na on the MoS_2/MoS_2 interface and (f) corresponding energy profiles along the diffusion path. Reproduced with permission.[71] Copyright 2013, Royal Society of Chemistry. (g and h) SEM and HRTEM images of D-MoS_2. (i) Schematic illustration of micro-channel defects and interlayer engineering to enhance K storage. Reproduced with permission.[72] Copyright 2019, Royal Society of Chemistry.

performed by Zheng *et al.*, the diffusion energy barrier of K ions at the MoS_2/MoS_2 interface with an interlayer spacing of 0.62 nm was 3.94 eV, and the diffusion barrier dramatically dwindled to 0.045 eV when the interlayer distance increased to 0.92 nm (Fig. 7f). It has been experimentally confirmed that expanding the interlayer spacing in MoS_2 could afford perdurable cycle stability with 1549 mA h g^{-1} after 500 cycles at a current density of 1000 mA g^{-1}.[71] However, it is not enough to fully utilize the special configuration of the van der Waals gap in MoS_2 only by expanding the interlamellar spacing to enhance K storage. Based on this point of view, Xu and colleagues combined defects in the basal planes and interlayer engineering to prepare interlayer-expanded and defect-rich MoS_2 nanoflowers (D-MoS_2 NFs) (Fig. 7g and h). As shown in Fig. 7i, the micro-channel defects generated in the basal surface can be K-ion intercalation sites to obtain more accessible interlayer spaces, and the extra edges with additionally exposed edge sites that are known to show fast response to Faraday and non-Faraday processes were created. Consequently, the capacity of D-MoS_2 NFs was 40% higher than the defect-free counterpart with the pristine interlayer spacing, which was attributed to the enhanced potassium ion insertion and diffusion and surface charge storage through the large interlayer spacing and in-plane defects.[72]

4 Summary and outlook

Research on electrochemical energy storage, especially in the field of materials science, is emerging with the increasing role of high-performance batteries as the major or backup power for electric vehicles and portable electronic devices, and extensive attention is being drawn to the exploitation of more efficient electrode materials. In the recent decade, the layered MoS_2 has attracted tremendous attention from academia due to its unique shape-dependent features and tunable physicochemical properties as an electrode material. In order to obtain better electrochemical performance, intensive efforts have been made to optimize the structure of MoS_2 material and regulate its physical and chemical properties through defect engineering. In this mini-review, the up-to-date research progress of defect engineering on MoS_2-based materials is summarized, from the characterization, categories and functions of defects to their promising application in various alkali metal ion batteries (Li, Na and K). This mini-review emphasizes the positive role of point-, line- and plane-like defect engineering in optimizing MoS_2-based electrode materials to achieve sustainable improvements for rechargeable battery applications. Recent reports on optimizing the electrochemical performance of MoS_2-based materials through defect engineering are summarized in Table 1.

Table 1 Comparison of the electrochemical performances of MoS_2-based electrode materials designed by defect engineering for the anode of alkali ion batteries from recent reports

Battery type	Electrodes	Defect categories	Current density (mA g^{-1})	Retention of capacity	Ref.
LIBs	N-Doped mesoporous molybdenum disulfide nanosheets	Heteroatoms doping	50	998 mA h g^{-1} after 100 cycles	57
LIBs	Nitrogen-doped MoS_2 nanosheets	Heteroatoms doping	134	1130.8 mA h g^{-1}	61
LIBs	Defect-rich $MoS_{2(1-x)}Se_{2x}$ few-layer nanocomposites	Heteroatoms doping	3350	500 mA h g^{-1} after 350 cycles	33
LIBs	Plasma-engineered MoS_2 nanosheets	O doping	1000	900 mA h g^{-1} for 1000 cycles	37
LIBs	Co-Doped-MoS_2/RGB hybrids	Heteroatoms doping	100	1223 mA h g^{-1} after 100 cycles	41
LIBs	Mn-Doped MoS_2 nanosheets anchored on C nanowire	Heteroatoms doping	1000	750 mA h g^{-1} over 1000 cycle	56
LIBs	Defect-enabled 3D porous MoS_2/C	S vacancy	100	1163 mA h g^{-1} after 100 cycles	38
LIBs	Edge-rich MoS_2 nanosheets anchored on curly N-doped graphene	Rich edge	500	675 mA h g^{-1} after 450 cycles	46
LIBs	MoS_2 nanosheets vertically grown on graphene sheets	High-exposed edge	1000	907 mA h g^{-1} after 400 cycles	64
LIBs	MoS_2/graphene/carbon composite	Exposed edge and expanded interlayer	5000	525 mA h g^{-1} after 1000 cycles	73
SIBs	Self-assembled N-doped MoS_2/carbon spheres	Doping and expanded interlayer	134	401 mA h g^{-1} after 200 cycles	35
SIBs	Nitrogen doped hollow MoS_2/C nanospheres	Doping and expanded interlayer	2000	128 mA h g^{-1} after 5000 cycles	36
SIBs	Co-doped 1T-MoS_2 nanosheets	Heteroatoms doping	5000	218.6 mA h g^{-1} after 8240 cycles	68
SIBs	Bundled defect-rich MoS_2	Vacancies	2000	350 mA h g^{-1} after 1000 cycles	32
SIBs	Hierarchical MoS_2 hollow architectures	Mo vacancies	1000	267 mA h g^{-1} after 125 cycles	74
SIBs	Supersaturated bridge-sulfur and vanadium co-doped MoS_2	Edge engineering and heteroatoms doping	2000	207 mA h g^{-1} after 3000 cycles	70
SIBs	The sandwich-type G@MoS_2-C	Expanded interlayer	3000	253 mA h g^{-1} after 4500 cycles	75
SIBs	MoS_2 nanosheets	Expanded interlayer	50	109 mA h g^{-1} after 100 cycles	66
SIBs	3D MoS_2/GNRA architecture	Expanded interlayer	5000	158 mA h g^{-1} after 1500 cycles	76
PIB	$MoS_{2(1-x)}Se_{2x}$ alloys	Anion vacancies	2000	220.5 mA h g^{-1} after 1000 cycles	51
PIB	Enriched edges MoS_2	Enriched edges	1000	321 mA h g^{-1} after 200 cycles	53
PIB	Interlayer-expanded MoS_2	Expanded interlayer	200	510 mA h g^{-1} after 100 cycles	48
PIB	Vertical MoS_2 nano-rose on graphene	Expanded interlayer	100	381 mA h g^{-1} after 100 cycles	77
PIB	Interlayer-expanded and defect-rich MoS_2 nanoflowers	Exposed edge and expanded interlayer	100	93.6 mA h g^{-1} after 100 cycles	72
PIB	Interlayer expanded MoS_2–N/O doped carbon composite	Expanded interlayer	1000	176 mA h g^{-1} after 500 cycles	71
PIB	Bamboo-like MoS_2/N-doped-C hollow tubes	Expanded interlayer	500	151 mA h g^{-1} after 1000 cycles	78

Despite the significant progress in this field, there are some challenges to be addressed.

A deeper understanding of the mechanism of defect engineering on MoS_2 electrode materials is still necessary and urgent. For example, the extrinsic defects, such as heteroatom doping at different positions, have a significant influence on charge redistribution and the band structure of the lamellar MoS_2. Hence, it is urgent to study the deep mechanism between the defect types and the changes in the electronic characteristics of the materials. Although it has been proved that defects such as heteroatom doping, vacancies, edge effects, and enlarging interlayer spacing in MoS_2 have a direct impact on ion transfer and adsorption, the structural evolution during the embeddedness and disembeddedness of foreign ions, the synergetic mechanism and individual contribution with multiple defects (such as doping and its induced interlayer extension) are completely unclear. In addition, based on the easy extension of the 2D topology in the MoS_2, the fundamental principles of electrochemical storage and conversion mechanisms enhanced by defect engineering for ions with different radii should be better investigated through theoretical calculations.

Secondly, the current characterization techniques for MoS_2 defects are unsatisfactory and ambiguous, limiting the research on defect-related mechanisms. Few characterizations and inspection methods can quantify defects. It is worth noting that the defect concentration in the electrode material is an important factor affecting its electronic structure and electrochemical performance. For example, the enhanced defect concentration can provide more accessible active sites for ions, but electron transport along the basic plane is significantly hindered due to the collapse of the 2D electron conjugation. Therefore, balancing the benefits between enriched active sites and excellent electrical conductivity is greatly important for the development of effective electrode materials by modulating the defect concentration. In addition, the ICE in the electrode materials mainly depends on the reversibility of the electrochemical reaction between surface defects and foreign ions. The conductivity and capacity can be improved to enhance the insertion/extraction reversibility by introducing certain defects

into the MoS_2 material, while the excessively high defect concentration will sacrifice the stability of the material. Hence, it is of significance to control moderate defect concentration for improving the ICE and maintaining cycle stability. Furthermore, some *in situ* techniques such as TEM, XRD, and XPS should be introduced to monitor the dynamic evolution of defects during the charge/discharge process of the battery, which provides direct evidence for the effects of induced defects and brings a new fundamental understanding of metal-ion storage mechanisms.

How defects affect the storage of guest ions such as ion adsorption and movement is revealed by the theoretical calculations, and the stable configuration after ion insertion is identified. This could further explain the extra capacity beyond the theoretical value based on the insertion/conversion mechanism. However, more theoretical calculations in MoS_2 electrodes are only a naive correlation calculation based on experimental results. Comprehensive theoretical calculations with different types of defects on the physicochemical properties should be performed to predict the impact on electrochemical performance, which can enhance the matching of experimental results and theoretical computations and provide guidance for research. In particular, the diffusion of ions with different radii in the MoS_2 body should be predicted in advance to screen suitable defect engineering through DFT calculations. There is no doubt that DFT calculation based on first principles is becoming increasingly significant to the analysis and forecasting of the strengthened effects of defects on MoS_2 electrodes employing rechargeable alkali metal-ion batteries. However, there are only single-layer or double-layer MoS_2 structure models for the adsorption energy and diffusion barrier calculation of guest ions on the surface of defect MoS_2, while the as-prepared layered MoS_2 is often multilayered (larger than the bilayer).[38] Also, the vacancy defects in real conditions are complicated, such as vacancy concentration and distribution.[40] Therefore, accurate theoretical structure models close to real circumstances should be constructed to more correctly calculate and simulate the enhanced effects induced by defects for electrochemical energy storage systems.

The positive role of defect engineering in MoS_2 electrode materials is summarized in this mini-review. Although there are some challenges to be fully overcome, the advancement of research and development of related technologies is inspiring us to overcome the existing deficiencies. Significant progress has been made in applications of the defect engineering of MoS_2-based materials in alkali metal-ion batteries, so integrating defects in MoS_2 materials to develop stable and efficient electrodes that can be applied to other energy storage and conversion fields is an extremely promising strategy. Hopefully, this mini-review will provide a deep understanding and draw attention to the design of advanced defective MoS_2 electrode materials, and considerably promote the development of the battery industry.

Conflicts of interest

There are no conflicts to declare.

Acknowledgements

This research was financially supported by the Hunan Provincial Science and Technology Plan Projects of China (No. 2020JJ2042, No. 2018RS3009 and No. 2017TP1001) and National Nature Science Foundation of China (No. 21975289).

References

1 S. Chu and A. Majumdar, Opportunities and challenges for a sustainable energy future, *Nature*, 2012, **488**, 294–303.
2 N. Kittner, F. Lill and D. M. Kammen, Energy storage deployment and innovation for the clean energy transition, *Nat. Energy*, 2017, **2**, 6.
3 M. D. Leonard, E. E. Michaelides and D. N. Michaelides, Energy storage needs for the substitution of fossil fuel power plants with renewables, *Renewable Energy*, 2020, **145**, 951–962.
4 C. Liu, F. Li, L. P. Ma and H. M. Cheng, Advanced materials for energy storage, *Adv. Mater.*, 2010, **22**, E28–E62.
5 J. B. Goodenough and Y. Kim, Challenges for rechargeable Li batteries, *Chem. Mater.*, 2010, **22**, 587–603.
6 M. Armand and J. M. Tarascon, Building better batteries, *Nature*, 2008, **451**, 652–657.
7 Y. J. Ma, Y. C. Zhang, S. S. Cai, Z. Y. Han, X. Liu, F. L. Wang, Y. Cao, Z. H. Wang, H. F. Li, Y. H. Chen and X. Feng, Flexible hybrid electronics for digital healthcare, *Adv. Mater.*, 2020, **32**, 23.
8 Y. Zhang, Y. Zhao, X. L. Cheng, W. Weng, J. Ren, X. Fang, Y. S. Jiang, P. N. Chen, Z. T. Zhang, Y. G. Wang and H. S. Peng, Realizing both high energy and high power densities by twisting three carbon-nanotube-based hybrid fibers, *Angew. Chem., Int. Ed.*, 2015, **54**, 11177–11182.
9 L. Li, Y. Zheng, S. L. Zhang, J. P. Yang, Z. P. Shao and Z. P. Guo, Recent progress on sodium ion batteries: potential high-performance anodes, *Energy Environ. Sci.*, 2018, **11**, 2310–2340.
10 H. S. Hou, X. Q. Qiu, W. F. Wei, Y. Zhang and X. B. Ji, Carbon anode materials for advanced sodium-ion batteries, *Adv. Energy Mater.*, 2017, **7**, 30.
11 T. Yuan, Z. P. Tan, C. R. Ma, J. H. Yang, Z. F. Ma and S. Y. Zheng, Challenges of spinel $Li_4Ti_5O_{12}$ for lithium-ion battery industrial applications, *Adv. Energy Mater.*, 2017, **7**, 25.
12 X. Wu, Y. L. Chen, Z. Xing, C. W. K. Lam, S. S. Pang, W. Zhang and Z. C. Ju, Advanced carbon-based anodes for potassium-ion batteries, *Adv. Energy Mater.*, 2019, **9**, 46.
13 D. Han, J. Zhang, Z. Weng, D. Kong, Y. Tao, F. Ding, D. Ruan and Q. Yang, Two-dimensional materials for lithium/sodium-ion capacitors, *Mater. Today Energy*, 2019, **11**, 30–45.
14 U. Gupta and C. N. R. Rao, Hydrogen generation by water splitting using MoS_2 and other transition metal dichalcogenides, *Nano Energy*, 2017, **41**, 49–65.
15 M. Chhowalla, D. Jena and H. Zhang, Two-dimensional semiconductors for transistors, *Nat. Rev. Mater.*, 2016, **1**, 15.

16 J. T. Xu, Y. H. Dou, Z. X. Wei, J. M. Ma, Y. H. Deng, Y. T. Li, H. K. Liu and S. X. Dou, Recent progress in graphite intercalation compounds for rechargeable metal (Li, Na, K, Al)-ion batteries, *Adv. Sci.*, 2017, **4**, 14.

17 J. Zhou, J. Qin, X. Zhang, C. Shi, E. Liu, J. Li, N. Zhao and C. He, 2D space-confined synthesis of few-layer MoS_2 anchored on carbon nanosheet for lithium-ion battery anode, *ACS Nano*, 2015, **9**, 3837–3848.

18 G. Jia, D. Chao, N. H. Tiepa, Z. Zhang and H. J. Fan, Intercalation Na-ion storage in two-dimensional $MoS_{2-x}Se_x$ and capacity enhancement by selenium substitution, *Energy Storage Mater.*, 2018, **14**, 136–142.

19 S. Dai, L. Wang, M. Cao, Z. Zhong, Y. Shen and M. Wang, Design strategies in metal chalcogenides anode materials for high-performance sodium-ion battery, *Mater. Today Energy*, 2019, **12**, 114–128.

20 Y. Hou, J. Li, Z. Wen, S. Cui, C. Yuan and J. Chen, N-doped graphene/porous g-C_3N_4 nanosheets supported layered-MoS_2 hybrid as robust anode materials for lithium-ion batteries, *Nano Energy*, 2014, **8**, 157–164.

21 M. Hu, H. Zhang, T. Hu, B. Fan, X. Wang and Z. Li, Emerging 2D MXenes for supercapacitors: status, challenges and prospects, *Chem. Soc. Rev.*, 2020, **49**, 6666–6693.

22 C. Chen, L. Tao, S. Q. Du, W. Chen, Y. Y. Wang, Y. Q. Zou and S. Y. Wang, Advanced exfoliation strategies for layered double hydroxides and applications in energy conversion and storage, *Adv. Funct. Mater.*, 2020, **30**, 18.

23 X. Qian, G. Zhu, K. Wang, F. Zhang, K. Liang, W. Luo and J. Yang, Bowl-like mesoporous polymer-induced interface growth of molybdenum disulfide for stable lithium storage, *Chem. Eng. J.*, 2020, **381**, 10.

24 Y. H. Li, K. Chang, E. Shangguan, D. Guo, W. Zhou, Y. Hou, H. Tang, B. Li and Z. Chang, Powder exfoliated MoS_2 nanosheets with highly monolayer-rich structures as high-performance lithium-/sodium-ion-battery electrodes, *Nanoscale*, 2019, **11**, 1887–1900.

25 A. H. Biby, B. A. Ali and N. K. Allam, Interplay of quantum capacitance with van der Waals forces, intercalation, co-intercalation, and the number of MoS_2 layers, *Mater. Today Energy*, 2021, **20**, 100677.

26 R. Zhang, Y. Qin, P. Liu, C. K. Jia, Y. Tang and H. Wang, How does molybdenum disulfide store charge: A minireview, *ChemSusChem*, 2020, **13**, 1354–1365.

27 Y. C. Jiao, A. Mukhopadhyay, Y. Ma, L. Yang, A. M. Hafez and H. L. Zhu, Ion transport nanotube assembled with vertically aligned metallic MoS_2 for high rate lithium-ion batteries, *Adv. Energy Mater.*, 2018, **8**, 9.

28 Y. W. Wang, L. Yu and X. Lou, Synthesis of highly uniform molybdenum-glycerate spheres and their conversion into hierarchical MoS_2 hollow nanospheres for lithium-ion batteries, *Angew. Chem., Int. Ed.*, 2016, **55**, 7423–7426.

29 Q. Li, H. Li, Q. Xia, Z. Hu, Y. Zhu, S. Yan, C. Ge, Q. Zhang, X. Wang, X. Shang, S. Fan, Y. Long, L. Gu, G.-X. Miao, G. Yu and J. S. Moodera, Extra storage capacity in transition metal oxide lithium-ion batteries revealed by in situ magnetometry, *Nat. Mater.*, 2021, **20**, 76–83.

30 Y. Yang, X. Liu, Z. Zhu, Y. Zhong, Y. Bando, D. Golberg, J. Yao and X. Wang, The role of geometric sites in 2D materials for energy storage, *Joule*, 2018, **2**, 1075–1094.

31 J. Wu, F. Ciucci and J.-K. Kim, Molybdenum disulfide based nanomaterials for rechargeable batteries, *Chem. – Eur. J.*, 2020, **26**, 6296–6319.

32 K. Yao, Z. Xu, J. Huang, M. Ma, L. Fu, X. Shen, J. Li and M. Fu, Bundled defect-rich MoS_2 for a high-rate and long-life sodium-ion battery: achieving 3D diffusion of sodium ion by vacancies to improve kinetics, *Small*, 2019, **15**, 1805405.

33 J. Wang, L. Zhang, K. Sun, J. He, Y. Zheng, C. Xu, Y. Zhang, Y. Chen and M. Li, Improving ionic/electronic conductivity of MoS_2 Li-ion anode via manganese doping and structural optimization, *Chem. Eng. J.*, 2019, **372**, 665–672.

34 Z. Fang, B. Bueken, D. E. De Vos and R. A. Fischer, Defect-engineered metal-organic frameworks, *Angew. Chem., Int. Ed.*, 2015, **54**, 7234–7254.

35 H. Lim, H. Kim, S.-O. Kim and W. Choi, Self-assembled N-doped MoS_2/carbon spheres by naturally occurring acid-catalyzed reaction for improved sodium-ion batteries, *Chem. Eng. J.*, 2020, **387**, 124144.

36 Y. Cai, H. Yang, J. Zhou, Z. Luo, G. Fang, S. Liu, A. Pan and S. Liang, Nitrogen doped hollow MoS_2/C nanospheres as anode for long-life sodium-ion batteries, *Chem. Eng. J.*, 2017, **327**, 522–529.

37 Y. Liu, L. Zhang, Y. Zhao, T. Shen, X. Yan, C. Yu, H. Wang and H. Zeng, Novel plasma-engineered MoS_2 nanosheets for superior lithium-ion batteries, *J. Alloys Compd.*, 2019, **787**, 996–1003.

38 K. Tao, X. Wang, Y. Xu, J. Liu, X. Song, C. Fu, X. Chen, X. Qu, X. Zhao and L. Gao, Engineering defect-enabled 3D porous MoS_2/C architectures for high performance lithium-ion batteries, *J. Am. Ceram. Soc.*, 2020, **103**, 4453–4462.

39 G. Barik and S. Pal, Defect induced performance enhancement of monolayer MoS_2 for Li- and Na-ion batteries, *J. Phys. Chem. C*, 2019, **123**, 21852–21865.

40 X. Sun, Z. Wang and Y. Q. Fu, Defect-Mediated Lithium Adsorption and Diffusion on Monolayer Molybdenum Disulfide, *Sci. Rep.*, 2015, **5**, 18712.

41 S. Xu, Q. Zhu, T. Chen, W. Chen, J. Ye and J. Huang, Hydrothermal synthesis of Co-doped-MoS_2/reduced graphene oxide hybrids with enhanced electrochemical lithium storage performances, *Mater. Chem. Phys.*, 2018, **219**, 399–410.

42 L. Zeng, F. Luo, X. Xia, M.-Q. Yang, L. Xu, J. Wang, X. Feng, Q. Qian, M. Wei and Q. Chen, An Sn doped 1T-2H MoS_2 few-layer structure embedded in N/P co-doped bio-carbon for high performance sodium-ion batteries, *Chem. Commun.*, 2019, **55**, 3614–3617.

43 X. Sun and Z. Wang, Adsorption and diffusion of lithium on heteroatom-doped monolayer molybdenum disulfide, *Appl. Surf. Sci.*, 2018, **455**, 911–918.

44 Y. Li, D. Wu, Z. Zhou, C. R. Cabrera and Z. Chen, Enhanced Li adsorption and diffusion on MoS_2 zigzag nanoribbons by edge effects: A computational study, *J. Phys. Chem. Lett.*, 2012, **3**, 2221–2227.

45 C. Uthaisar and V. Barone, Edge effects on the characteristics of Li diffusion in graphene, *Nano Lett.*, 2010, **10**, 2838–2842.
46 Q. Xia and Q. Tan, Towel-like composite: Edge-rich MoS_2 nanosheets oriented anchored on curly N-Doped graphene for high-performance lithium and sodium storage, *Electrochim. Acta*, 2019, **308**, 217–226.
47 K. D. Rasamani, F. Alimohammadi and Y. Sun, Interlayer-expanded MoS_2, *Mater. Today*, 2017, **20**, 83–91.
48 S. Di, P. Ding, Y. Wang, Y. Wu, J. Deng, L. Jia and Y. Li, Interlayer-expanded MoS_2 assemblies for enhanced electrochemical storage of potassium ions, *Nano Res.*, 2020, **13**, 225–230.
49 Y. Jia, K. Jiang, H. T. Wang and X. D. Yao, The role of defect sites in nanomaterials for electrocatalytic energy conversion, *Chem*, 2019, **5**, 1371–1397.
50 B. Chen, E. Liu, T. Cao, F. He, C. Shi, C. He, L. Ma, Q. Li, J. Li and N. Zhao, Controllable graphene incorporation and defect engineering in MoS_2–TiO_2 based composites: Towards high-performance lithium-ion batteries anode materials, *Nano Energy*, 2017, **33**, 247–256.
51 G. Cai, L. Peng, S. Ye, Y. Huang, G. Wang and X. Zhang, Defect-rich $MoS_{2(1-x)}Se_{2x}$ few-layer nanocomposites: a superior anode material for high-performance lithium-ion batteries, *J. Mater. Chem. A*, 2019, **7**, 9837–9843.
52 H. He, D. Huang, G. Gan, J. Hao, S. Liu, Z. Wu, W. K. Pang, B. Johannessen, Y. Tang, J. L. Luo, H. Wang and Z. Guo, Anion vacancies regulating endows MoSSe with fast and stable potassium ion storage, *ACS Nano*, 2019, **13**, 11843–11852.
53 Z. Zhang, S. Wu, J. Cheng and W. Zhang, MoS_2 nanobelts with (002) plane edges-enriched flat surfaces for high-rate sodium and lithium storage, *Energy Storage Mater.*, 2018, **15**, 65–74.
54 J. Jiang, X. Xu, H. Han, C. Qu, H. Repich, F. Xu and H. Wang, Edge-enriched MoS_2 for kinetics-enhanced potassium storage, *Nano Res.*, 2020, **13**, 2763–2769.
55 C. Tsai, H. Li, S. Park, H. S. Han, J. K. Nørskov, X. Zheng and F. Abild-Pedersen, Electrochemical generation of sulfur vacancies in the basal plane of MoS_2 for hydrogen evolution, *Nat. Commun.*, 2017, **8**, 15113.
56 J. Liang, Z. Wei, C. Wang and J. Ma, Vacancy-induced sodium-ion storage in N-doped carbon Nanofiber@MoS_2 nanosheet arrays, *Electrochim. Acta*, 2018, **285**, 301–308.
57 S. Qin, W. Lei, D. Liu and Y. Chen, Advanced N-doped mesoporous molybdenum disulfide nanosheets and the enhanced lithium-ion storage performance, *J. Mater. Chem. A*, 2016, **4**, 1440–1445.
58 B. Chen, E. Liu, F. He, C. Shi, C. He, J. Li and N. Zhao, 2D sandwich-like carbon-coated ultrathin TiO_2@defect-rich MoS_2 hybrid nanosheets: Synergistic-effect-promoted electrochemical performance for lithium ion batteries, *Nano Energy*, 2016, **26**, 541–549.
59 B. Chen, H. Lu, N. Zhao, C. Shi, E. Liu, C. He and L. Ma, Facile synthesis and electrochemical properties of continuous porous spheres assembled from defect-rich, interlayer-expanded, and few-layered MoS_2/C nanosheets for reversible lithium storage, *J. Power Sources*, 2018, **387**, 16–23.
60 Y. Wang, M. Zhen, H. Liu and C. Wang, Interlayer-expanded MoS_2/graphene composites as anode materials for high-performance lithium-ion batteries, *J. Solid State Electrochem.*, 2018, **22**, 3069–3076.
61 Q. Liu, W. Xia, Z. Wu, J. Huo, D. Liu, Q. Wang and S. Wang, The origin of the enhanced performance of nitrogen-doped MoS_2 in lithium ion batteries, *Nanotechnology*, 2016, **27**, 175402.
62 L. Lu, F. Min, Z. Luo, S. Wang, F. Teng, G. Li and C. Feng, Synthesis and electrochemical properties of tin-doped MoS_2 (Sn/MoS_2) composites for lithium ion battery applications, *J. Nanopart. Res.*, 2016, **18**, 357.
63 K. Qj, Z. Yuan, Y. Hou, R. Zhao and B. Zhang, Facile synthesis and improved Li-storage performance of Fe-doped MoS_2/reduced graphene oxide as anode materials, *Appl. Surf. Sci.*, 2019, **483**, 688–695.
64 Y. Teng, H. Zhao, Z. Zhang, Z. Li, Q. Xia, Y. Zhang, L. Zhao, X. Du, Z. Du and P. Lv, and K. Świerczek, MoS_2 Nanosheets Vertically Grown on Graphene Sheets for Lithium-Ion Battery Anodes, *ACS Nano*, 2016, **10**, 8526–8535.
65 T. Wang, S. Chen, H. Pang, H. Xue and Y. Yu, MoS_2-Based Nanocomposites for Electrochemical Energy Storage, *Adv. Sci.*, 2017, **4**, 1600289.
66 C. Zhao, C. Yu, B. Qiu, S. Zhou, M. Zhang, H. Huang, B. Wang, J. Zhao, X. Sun and J. Qiu, Ultrahigh Rate and Long-Life Sodium-Ion Batteries Enabled by Engineered Surface and Near-Surface Reactions, *Adv. Mater.*, 2018, **30**, 1702486.
67 H. Dong, Y. Xu, C. Zhang, Y. Wu, M. Zhou, L. Liu, Y. Dong, Q. Fu, M. Wu and Y. Lei, MoS_2 nanosheets with expanded interlayer spacing for enhanced sodium storage, *Inorg. Chem. Front.*, 2018, **5**, 3099–3105.
68 P. Li, Y. Yang, S. Gong, F. Lv, W. Wang, Y. Li, M. Luo, Y. Xing, Q. Wang and S. Guo, Co-doped 1T-MoS_2 nanosheets embedded in N, S-doped carbon nanobowls for high-rate and ultra-stable sodium-ion batteries, *Nano Res.*, 2019, **12**, 2218–2223.
69 J. Wang, Q. Zhao and J. Chen, Edge engineering of MoS_2 nanoribbons as high performance electrode material for Na-ion battery: A first-principle study, *Chin. J. Chem.*, 2017, **35**, 896–902.
70 Y. Dong, Z. Zhu, Y. Hu, G. He, Y. Sun, Q. Cheng, I. P. Parkin and H. Jiang, Supersaturated bridge-sulfur and vanadium co-doped MoS_2 nanosheet arrays with enhanced sodium storage capability, *Nano Res.*, 2021, **14**, 74–80.
71 N. Zheng, G. Jiang, X. Chen, J. Mao, Y. Zhou and Y. Li, Rational design of a tubular, interlayer expanded MoS_2-N/O doped carbon composite for excellent potassium-ion storage, *J. Mater. Chem. A*, 2019, **7**, 9305–9315.
72 Y. Xu, F. Bahmani, M. Zhou, Y. Li, C. Zhang, F. Liang, S. H. Kazemi, U. Kaiser, G. Meng and Y. Lei, Enhancing potassium-ion battery performance by defect and interlayer engineering, *Nanoscale Horiz.*, 2019, **4**, 202–207.

73 L. Zhang, Y. Pan, Y. Chen, M. Li, P. Liu, C. Wang, P. Wang and H. Lu, Designing vertical channels with expanded interlayers for Li-ion batteries, *Chem. Commun.*, 2019, **55**, 4258–4261.

74 Y. Li, R. Zhang, W. Zhou, X. Wu, H. Zhang and J. Zhang, Hierarchical MoS_2 hollow architectures with abundant Mo vacancies for efficient sodium storage, *ACS Nano*, 2019, **13**, 5533–5540.

75 C. Zhao, C. Yu, B. Qiu, S. Zhou, M. Zhang, H. Huang, B. Wang, J. Zhao, X. Sun and J. Qiu, Ultrahigh Rate and Long-Life Sodium-Ion Batteries Enabled by Engineered Surface and Near-Surface Reactions, *Adv. Mater.*, 2018, **30**, 1702486.

76 Y. Liu, X. Wang, X. Song, Y. Dong, L. Yang, L. Wang, D. Jia, Z. Zhao and J. Qiu, Interlayer expanded MoS_2 enabled by edge effect of graphene nanoribbons for high performance lithium and sodium ion batteries, *Carbon*, 2016, **109**, 461–471.

77 K. Xie, K. Yuan, X. Li, W. Lu, C. Shen, C. Liang, R. Vajtai, P. Ajayan and B. Wei, Superior Potassium Ion Storage via Vertical MoS_2 ''Nano-Rose'' with Expanded Interlayers on Graphene, *Small*, 2017, **13**, 1701471.

78 B. Jia, Q. Yu, Y. Zhao, M. Qin, W. Wang, Z. Liu, C.-Y. Lao, Y. Liu, H. Wu, Z. Zhang and X. Qu, Bamboo-Like Hollow Tubes with MoS2/N-Doped-C Interfaces Boost Potassium-Ion Storage, *Adv. Funct. Mater.*, 2018, **28**, 1803409.

